

Measurement of the Thermal Conductivity of Individual Carbon Nanotubes by the Four-Point Three- ω Method

Tae-Youl Choi,[†] Dimos Poulikakos,^{*,†} Joy Tharian,[‡] and Urs Sennhauser[‡]

Laboratory of Thermodynamics in Emerging Technologies, ETH, Zurich, Switzerland,
and Electronics/Metrology Laboratory, EMPA, Zurich, Switzerland

Received February 13, 2006; Revised Manuscript Received June 15, 2006

ABSTRACT

The thermal conductivity of individual multiwalled carbon nanotubes was measured by utilizing the four-point-probe third-harmonic method, based on the fact that the third harmonic amplitude and phase as a response to applied alternate current at fundamental frequency, ω , can be expressed in terms of thermal conductivity and diffusivity. To this end, a microfabricated device composed of four metal electrodes was modified to manufacture nanometer-sized wires by using a focused ion beam source. A carbon nanotube could then be suspended over a deep trench milled by the focused ion beam, preventing heat loss to the substrate. Compared with the two-point-probe technique, a significant improvement in accuracy is assured by using four probes, because the contact contribution to the determination of the thermal conductivity is eliminated, making it possible to measure the correct signals of first and third harmonics. The multiwalled carbon nanotube was modeled as a one-dimensional diffusive energy transporter and its thermal conductivity was measured at room temperature under vacuum to be 300 ± 20 W/mK.

Theories^{1,2} and experiments^{3–6} showed that carbon nanotubes have remarkable thermal properties. However, both the experimental data and the theoretical predictions are scattered over 1 order of magnitude. For example, in recent experiments^{4,6} the reported thermal conductivities for multiwalled carbon nanotubes at room temperature are in the range 400–3000 W/mK, likely depending on the type and size of carbon nanotubes (CNTs) utilized, which give rise to different mean free paths of the energy carriers. There is still a need for a reliable and reproducible measurement technique to test the theoretical predictions and to provide fundamental thermophysical data for an efficient design of carbon nanotube based nanoelectronics. To fully understand the fundamental heat transport characteristics in the mesoscopic scale, reliable data of thermal conductivity for various sizes of nanotubes should be collected in a reasonably precise manner. To this end, we developed a novel measurement technique based on the four-point-probe third-harmonic ($3-\omega$) method with assistance of a focused ion beam (FIB) source for the fabrication of the needed experimental device.

The thermal conductivity of individual carbon nanotubes or bundles of single-walled CNTs has been recently measured

by utilizing the “thermal conductance” technique^{4,6} and the “ $3-\omega$ ” method.^{5,7} A previous study⁵ showed that the multiwalled carbon nanotubes (MWCNTs) with diameter of about 40 nm have a dissipative nature, in which a one-dimensional transient heat transport equation can be used to derive the third harmonic voltage expression as a function of thermal conductivity. Since the measurement platform in ref 5 provided only two probes, there remains an uncertainty in the measurement of the true dc resistance, which contributes to power dissipation along the nanotube. In the two-point probe method, the contact resistance cannot be completely eliminated with certainty. This contact resistance is often included in the resistance measurement. Even though at a certain frequency an ac current can short circuit the capacitance in the electrical network between the nanotube and the metal contacts and, thus, the contact resistance can have no effect on the third harmonic signal,⁵ it will be a source of errors in the calculation of thermal conductivity since the thermal conductivity depends on the dc resistance. Moreover, a careful selection of frequency range is necessary, which can be accomplished by two-point and four-point probe measurements.

In the current study, we have developed the four-point $3-\omega$ method for a carbon nanotube. However, the proposed method can be easily implemented to other nanosystems. With this method, the contact resistance was eliminated and

* To whom correspondence should be addressed. E-mail: dimos.poulikakos@lnt.tet.mavt.ethz.ch.

[†] Laboratory of Thermodynamics in Emerging Technologies, ETH.

[‡] Electronics/Metrology Laboratory, EMPA, Zurich, Switzerland.

spurious signals caused by it could be avoided. Hence, the contact contribution can be neglected in both the electrical and the thermal network. To construct a four-wire connection, a simple nanofabrication process was developed in which FIB milling was performed on a prefabricated microdevice. The control of individual carbon nanotubes was realized by dielectrophoresis.^{5,8} By applying a constant amplitude ac current through the carbon nanotube, we could generate a temperature rise fluctuating at the second harmonic and measure the 3ω signal, which is used to compute the thermal conductivity. The multiwalled carbon nanotube used in this study shows a dissipative nature.

MWCNTs are diffusive conductors.^{9–12} A study with scanning thermal microscopy (SThM) pointed out the diffusive nature of MWCNTs, represented by the temperature gradient along the nanotube.⁹ This diffusive behavior is shown in a recent electrostatic microscopy study.³ As a consequence, the one-dimensional heat diffusive equation along the nanotube suspended between two metal electrodes can be utilized to obtain a closed form solution of the third harmonic response as shown in eq 1

$$\rho c_p \frac{\partial T}{\partial t} - k \frac{\partial^2 T}{\partial x^2} = \frac{I_0^2 \sin^2 \omega t}{LS} [R_0 + R'(T - T_0)] \quad (1)$$

where, L , R [$=R_0 + R'(T - T_0)$], and S are length, electrical resistance, and cross sectional area of the CNTs, respectively. R' is the temperature gradient of the resistance at room temperature defined as $(dR/dT)_{T_0}$. The initial and boundary conditions for the temperature are room temperatures (T_0) at time = 0 and at the contacts between the CNT and the metal electrodes. By solving for the temperature field fluctuating at the second harmonic frequency (the resistance fluctuation is at the same frequency), one can obtain the third harmonic response of the system with an accuracy of 1.2% when the condition, $I_0^2 R' L / n^2 \pi^2 k S \ll 1$ is met.⁷

$$V_{3\omega, \text{rms, vac}} \cong \frac{\sqrt{2} I_0^3 R R' L}{\pi^4 k S} \quad (2)$$

To satisfy this condition, the input current should be kept as low as possible to increase the measurement accuracy and avoid spurious signals caused by the possible heat generation at the contacts leading to change of boundary conditions. The maximum current amplitude depends on the resistance of the sample. Typically, the input current is limited to 10 μA (when $R \sim 10 \text{ k}\Omega$) or several tens of μA (when $R \sim 1 \text{ k}\Omega$).

Figure 1 shows a schematic diagram of the experimental setup. The lock-in amplifier (Stanford Research System SR 850) was used to pick up the 3ω signal by amplifying the small voltage ($\sim \mu\text{V}$) and removing the noise. The lock-in parameters for measuring such a small signal should be carefully selected in order to obtain stable signals with minimum noise. In the current study, 500 μV full scale and maximum dynamic reserve were set in the instrument. Since the working frequency for the sample in this study is 1000

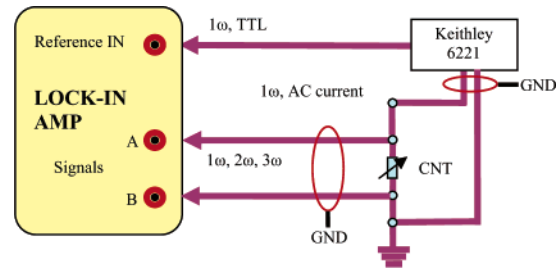


Figure 1. Schematic diagram of the measurement setup. The third harmonic signal generated in the specimen is measured, due to the fundamental ac current excitation. A precisely controlled ac current source is used to prevent voltage overshoot, which can damage the CNT sample.

Hz, 3 s of time constant is sufficient for stability. Regarding current supply, one can use a simple operation amplifier and a resistor for a constant current source for the measurement of a Pt microwire.⁷ For the measurement of CNT, a more precise and very well controlled current source (with minimum overshoot) must be employed because the carbon nanotubes can be damaged due to the high current density caused by the overshoot. A Keithley 6221 fits well into this category of current sources. To control and place a CNT across designated electrodes as shown in Figure 2b, a microdevice that has four electrical contacts was prefabricated by the lift-off technique (not shown in the figure). The electrical contacts were then modified by using FIB. Figure 2a depicts four nanofabricated electrodes. The two electrodes at the ends (labeled 1 and 4 in the figure) were milled in a round shape to increase the yield in the deposition of CNT along the electrodes. The deep trench (depth of over 1 μm) was made in the middle of the contacts. This effectively prevents the nanotube from touching the substrate. If it touches the substrate, electrical and/or thermal insulation will not be ensured, leading to short circuit with the substrate (for a Si substrate) or change of boundary condition (for Si and/or dielectric substrates).

The next step is to position a commercially available carbon nanotube purchased from Nanolab, Inc., USA (Figure 2b). A detailed procedure of deposition was explained in a previous study.⁵ One aspect to note is that the preparation of the carbon nanotube solution with correct concentration and cleanliness is crucial for the success of placement of individual carbon nanotubes. One milligram of carbon nanotube powder was mixed with 3 mL of pure ethanol. This solution (a seed solution) is then sonicated for a few minutes to disperse the nanotubes homogeneously. Only 5 μL of this seed solution is dispensed into 25 mL of ethanol. The successively diluted solution was ensured to maintain the cleanliness and proper concentration. The diluted solution was finally sonicated for about 5 h. The yield for the deposition of individual carbon nanotubes turned out to be poor ($< 10\%$) in this study because the size of nanotubes in the solution ranges from 15 to 45 nm. Another cause is due to the electrical interference between the round and straight electrodes; the electric field is applied between the round electrodes.

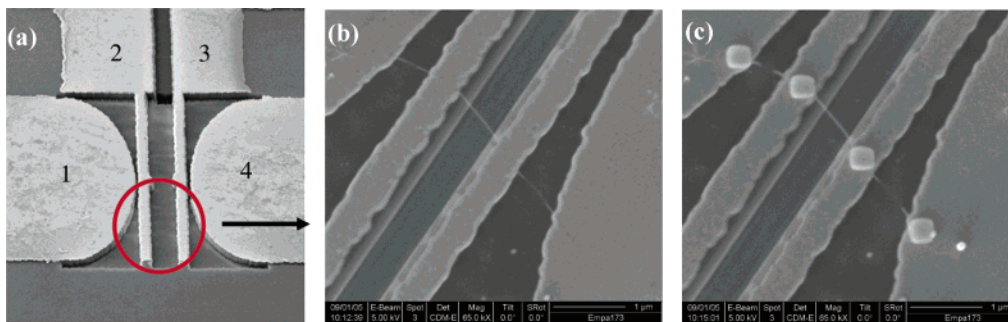


Figure 2. A series of pictures of a four-point-probe $3-\omega$ experiment: (a) four-wire construction by focused ion beam milling; (b) selective deposition of single CNT by dielectrophoresis; (c) electron beam soldering at four contacts.

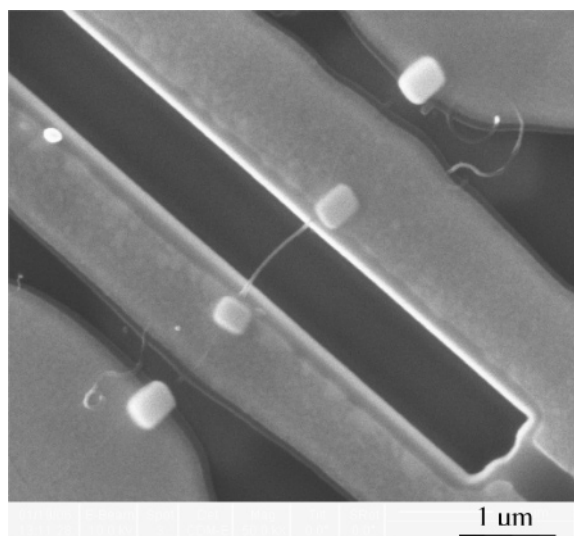


Figure 3. Single carbon nanotube deposited along the four metal contacts. The outer diameter of the nanotube is measured at 20 nm and the inner diameter is estimated at 10 nm. The deep trench made by FIB with a depth of over $1\ \mu\text{m}$ prevents the nanotube from touching the substrate (Si in this study).

Once the deposited carbon nanotube is located along the four metal electrodes, the four contacts between the nanotube and metal pads can be soldered by electron beam assisted Pt deposition in the dual beam FIB chamber (FEI Strata 400) as shown in Figure 2c. In this manner, the contact resistance can be greatly reduced. Further annealing at $550\ ^\circ\text{C}$ has been performed to almost eliminate the contact resistance.¹³

Figure 3 shows another sample prepared by the aforementioned procedure. The nanotube diameter was measured at $20 \pm 1.2\ \text{nm}$ of outer diameter with ultrahigh resolution in the SEM. An inner diameter of 10 nm is estimated from TEM pictures provided by the supplier (Nanolab, Inc., USA). The length of the tube along the trench is measured at $1.4\ \mu\text{m}$. All the measurements including resistance, temperature, and $3-\omega$ signals were made in a vacuum at $6 \times 10^{-3}\ \text{mbar}$.

The resistance was measured in the temperature range of $24.8\text{--}27.9\ ^\circ\text{C}$, which is close to the measurement temperature of the $3-\omega$ signal (Figure 4). dc resistance was obtained since only the real component of the impedance contributes to the power dissipation. The carbon nanotube sample was placed on the calibration block, which is composed of a thermometer and a heater. To measure accurately, the entire

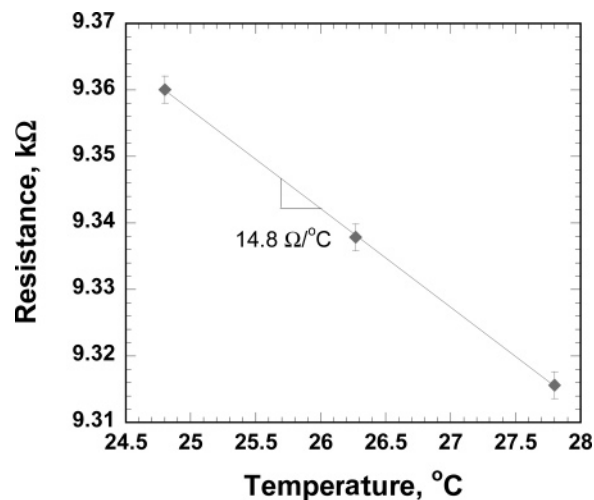


Figure 4. dc resistance at $T = 24.4\text{--}27.9\ ^\circ\text{C}$. The measured data reveal a linearly decreasing value as the temperature rises, as expected. The calculated temperature coefficient is $-14.8\ \Omega/^\circ\text{C}$.

block was covered by a radiation shield which is also maintained at the same temperature of the block. The resistance and the temperature coefficient of the sample were measured at $9.36\ \text{k}\Omega$ and $-14.8\ \Omega/^\circ\text{C}$ at $T = 24.4\ ^\circ\text{C}$. It should be noted that the highest possible current was applied to maximize the resolution of the measurement with no self-heating effect. By applying nearly zero current (100 pA), the electrical wire junctions were examined to make sure that no thermocouple voltage is generated. The contact contribution to possible generation of artifacts is thoroughly examined by two- and four-point dc resistance measurements and by an ac impedance spectroscopy study. The contact contribution has both an electrical and a thermal effect. When the electrical contact resistance is too high, the measured third harmonics will be affected by the heat dissipation that occurs at the contacts due to the Joule heating. Incorrect selection of a working frequency will result in a misinterpretation of experimental results. The heat dissipation at the contacts due to the electrical contact resistance turned out to be negligible for the entire range of current excitation. The ac impedance measurements were used to select a correct working frequency with which no electrical artifacts are involved.

The contact resistance gives rise in general to a spurious signal in measuring the $3-\omega$ voltage. In addition, it results

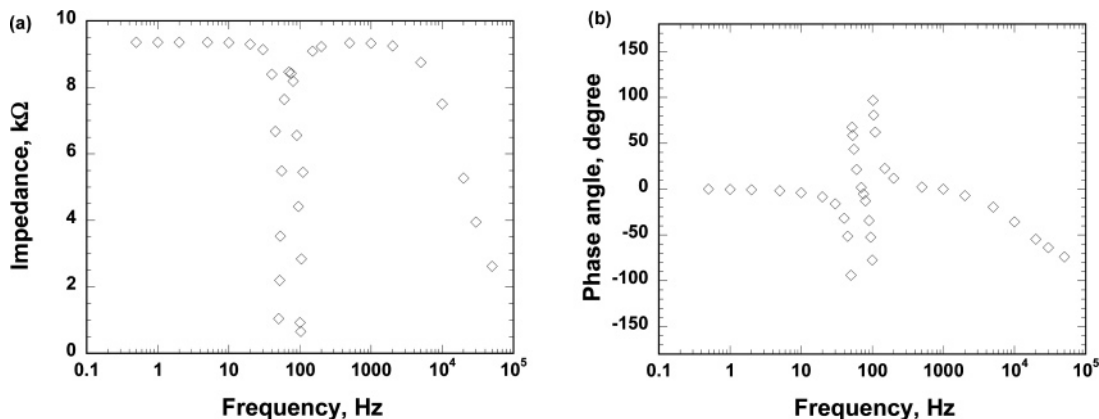


Figure 5. Impedance spectrum for the carbon nanotube in Figure 2c measured with four-wire configuration in the frequency range of 0.5–50000 Hz. Two resonance points are indicated at 50 and 100 Hz.

in an uncertainty in the measurement of true dc resistance (which is responsible for the 3ω signal) and in possible boundary condition changes. Depending on the type of the outermost shell of the CNT, the contact can be Schottky or ohmic. The sample used in this study showed nearly ohmic contacts. By applying the known dc current between the contacts 1 and 4 and measuring the voltage drop across 2 and 3 (in Figure 2a), one can determine the resistance of the contacts and the test section. The resistance by the two-point probe configuration is expressed as $R_{2point} = R_{lead} + 2R_{cont} + R_{CNT}$. Measuring R_{2point} and R_{CNT} by two- and four-point probes and neglecting R_{lead} ($\sim 10 \Omega$ in this study), we obtain the contact resistance as $R_{cont} = (R_{2point} - R_{CNT})/2$, which turned out to be about 8% of R_{CNT} . The contact resistance measured in this study will not affect the third harmonic signal because of the low current excitation (the maximum power dissipation at the contacts is much smaller than the minimum power for the 3ω signal). Additionally, the contact metal pads are large thermal reservoirs in which the temperature is fixed at the initial temperature at all conditions of experiment.

The carbon nanotube is modeled as a resistance, capacitor, and an inductor which are connected in parallel. The four-point-probe spectroscopic measurement of impedance is shown in Figure 5. In the frequency range of 0.5–3000 Hz, the impedance stays nearly constant except for the two resonance points, suggesting that capacitance and inductance have no notable effect on the impedance measurement. In fact, geometrical inductance and capacitance for a long coil with radius of 10 nm and length of $1 \mu\text{m}$ can be estimated to be of the order of 100 pH and 0.1 fF, respectively,¹⁴ which does not contribute to the total impedance in the frequency range of this study. Regardless of the wire configuration, there exist two resonance points at 50 and 100 Hz, implying that they are not originated from intrinsic capacitance or inductance. A possible cause is due to the interference with the wall outlet power. The parasitic capacitance effect caused by the dielectric film (SiN in this case) appears to be evident at frequencies over 5000 Hz. From this measurement, one can ensure that no electrical parasitic artifacts appear in a certain range of working frequency and the present work was performed in this range.

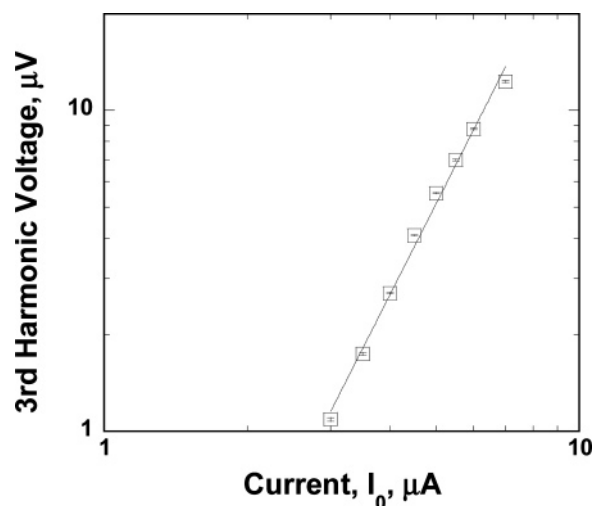


Figure 6. Measured 3ω signal as a function of input current. The measurement was achieved at a working frequency of 1000 Hz. The exponent obtained by best fitting is 2.9, which complies with the prediction.

At room temperature of $24.4 \text{ }^\circ\text{C}$, the 3ω signal was measured at the frequency of 1000 Hz. The working frequency was selected by ensuring that there exist no artifacts (as presented in the frequency range of 500–3000 Hz) and possible high-frequency noises are prevented. At the frequency of 1000 Hz, the four-point-probe ac resistance turned out to be close to its dc counterpart (within 0.1%, compare Figures 4 and 7), rendering a correct interpretation of heat dissipation at this frequency.

The 3ω signal starts appearing at $3 \mu\text{A}$ (Figure 6). The starting current is relatively low as compared to the previous study⁵ due to the high resistance of the sample. The signal follows well the predicted third power law as shown in eq 2. The exponent from the best fit of the measured points is 2.9, being very close to the third power. It can be concluded that the employed sample in the current study also shows a dissipative nature. Using eq 2, one can calculate the thermal conductivity of the sample from the measured 3ω signal, resistance, temperature coefficient, length, and the CNT diameters. Averaging the calculated data, the thermal conductivity is obtained to be $300 \pm 20 \text{ W/mK}$. This measured value is 1 order of magnitude smaller than that of single-

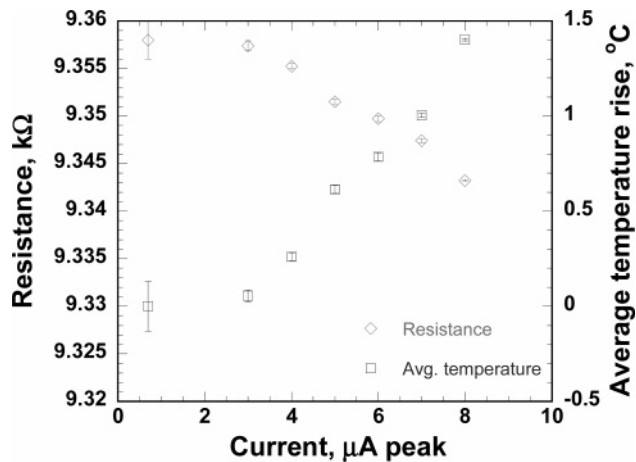


Figure 7. Measured resistance as a function of current and calculated average temperature rise along the sample at $T = 24.4\text{ }^{\circ}\text{C}$ and at $f = 1000\text{ Hz}$. The relationship between the current and resistance for most of the range is approximately linear.

walled carbon nanotube predicted by theory.² Possible causes of lower thermal conductivity from multiwall CNTs are the intertubular scattering of phonons and anharmonic scattering process (Umklapp process), which is the dominant scattering mechanism at room temperature. This process occurs within the mean free path of phonons.¹³ Assuming that the group velocity of phonons and specific heat of a CNT are $\sim 20000\text{ m/s}$ ¹⁶ and $\sim 1000\text{ kJ}/(\text{m}^3\text{ K})$,^{7,17} respectively, one can estimate the phonon mean free path with the relation, $k = \frac{1}{3}c_p v l$ derived from the classical kinetic theory. The estimated value is at around 50 nm . In this case, the local temperature along the specimen can be defined since the characteristic length ($1.4\text{ }\mu\text{m}$) is much larger than the mean free path of the energy carriers. So, heat flow through the MWCNT is diffusive, which agrees with the prediction.

The measured resistance at the working frequency of 1000 Hz as a function of input current is shown in Figure 7. The substrate temperature is set at $24.4\text{ }^{\circ}\text{C}$. Another representation of this figure is the I - V characteristic, since the measured signal is the voltage. The I - V characteristic shows deviation from a linear trend (in other words constant resistance) beyond $3\text{ }\mu\text{A}$, which coincides with the incipience of the $3\text{-}\omega$ signal. It is interesting to note that the average temperature rise along the CNT is a couple of degrees at $7\text{ }\mu\text{A}$. This implies that the $3\text{-}\omega$ measurement is very sensitive to a small temperature fluctuation and that the temperature of the specimen did not greatly deviate from the substrate temperature, which excludes the possibility of the artifact due to the high-temperature rise along the sample. It should be noted that in this temperature rise, the radiation loss due to the fluctuation of the temperature can be neglected. The

errors involved with the measurement are summarized as follows: 0.03% for resistance, 2% for length, 6% for diameter, 2% for $3\text{-}\omega$ voltage. The total estimated error falls within $\pm 7\%$.

In summary, we introduced a novel method to characterize the thermal and electrical properties of a suspended individual nanostructure, which can be a great interest to nanotechnology in terms of control and characterization of nanosystem components. It was shown that the thermal conductivity of individual multiwalled carbon nanotubes can be obtained by the four-point-probe $3\text{-}\omega$ method. As compared to the two-point probe $3\text{-}\omega$ method, the accuracy of the measurement is significantly enhanced by eliminating the contact contribution in the measurement. The measured value for the CNTs investigated in this paper is $300 \pm 20\text{ W/mK}$. The dissipative nature of phonon transport has been verified with the measurement of $3\text{-}\omega$ signal, which follows the third power law.

Acknowledgment. This research was supported in part by a research grant of the Research Commission of ETH Zurich.

References

- (1) Berber, S.; Kwon, Y.; Tomanek, D. *Phys. Rev. Lett.* **2000**, *84*, 4613.
- (2) Che, J.; Cagin, T.; Goddard III, W. A. *Nanotechnology* **2000**, *11*, 65.
- (3) Bachtold, A.; Fuhrer, M. S.; Plyasunov, S.; Forero, M.; Anderson, E. H.; Zettl, A.; McEuen, P. *Phys. Rev. Lett.* **2000**, *84*, 6082.
- (4) Kim, P.; Shi, L.; Majumdar, A.; McEuen, P. *Phys. Rev. Lett.* **2001**, *87*, 215502.
- (5) Choi, T.; Poulidakos, D.; Tharian, J.; Sennhauser, U. *Appl. Phys. Lett.* **2005**, *87*, 013108.
- (6) Fujii, M.; Zhang, X.; Xie, H.; Ago, H.; Takahashi, K.; Ikuta, T.; Abe, H.; Shimizu, T. *Phys. Rev. Lett.* **2005**, *95*, 065502.
- (7) Yi, W.; Lu, L.; Dian-lin, Z.; Pan, Z. W.; Xie, S. *Physical Review B* **1999**, *59*, R9015.
- (8) Chung, J.; Lee, K.; Lee, J.; Ruoff, R. S. *Langmuir* **2004**, *20*, 3011.
- (9) Shi, L. *Mesososcopic thermophysical measurement of microstructures and carbon nanotubes*, Ph.D. Thesis, UC Berkeley, 2001, 80.
- (10) Bachtold, A.; Strunk, C.; Salvetat, J.-P.; Bonard, J.-M.; Forro, L.; Nussbaumer, T.; Schönengerger, C. *Nature* **1999**, *397*, 673.
- (11) Langer, L.; Bayot, V.; Grivei, E.; Issi, J.-P.; Heremans, J. P.; Olk, C. H.; Stockman, L.; Van Haesendonck, C.; Bruynseraede, Y. *Phys. Rev. Lett.* **1996**, *76*, 479.
- (12) Schönengerger, C.; Bachtold, A.; Strunk, C.; Salvetat, J.-P.; Forro, L. *Appl. Phys. A* **1999**, *69*, 283.
- (13) Gopal, V.; Radmilovic, V. R.; Daraio, C.; Yang, J. P.; Stach, E. A. *Nanoletters* **2004**, *4*, 2059.
- (14) Y. P. Zhao, B. Q. Wei, P. M. Ajayan, G. Ramanath, T. M. Lu, G. C. Wang, A. Rubio, and S. Roche, *Phys. Rev. B* **2001**, *64*, 201402–1.
- (15) Cahill, D.; Ford, W.; Goodson, K.; Mahan, G.; Majumdar, A.; Maris, H.; Merlin, R.; Phillpot, S. *J. of Appl. Phys.* **2003**, *93*, 793.
- (16) Hone, J.; Llaguno, M. C.; Biercuk, M. J.; Johnson, A. T.; Batlogg, B.; Benes, Z.; Fischer, J. E. *Appl. Phys. A* **2002**, *74*, 339.
- (17) Jishi, R.; Venkataraman, L.; Dresselhaus, M.; Dresselhaus, G. *Chem. Phys. Lett.* **1993**, *209*, 77.

NL060331V